Int. J. Nanosci. Nanotechnol., Vol. 8, No. 3, Sep. 2012, pp. 157-164

Synthesis of MgO Nanoparticales and Identification of Their Destructive Reaction Products by 2-Chloroethyl Ethyl Sulfide

B. Maddah*, H. Chalabi

Department of Chemistry, Imam Hossein University, Tehran, I. R. Iran

(*) Corresponding author: bozorgmaddah@yahoo.com
(Received:02 Aug. 2012 and Accepted: 20 Sep. 2012)

Abstract:
Nanocrystalline magnesium oxides were prepared by sol–gel method and were characterized by X-ray diffraction, N_2-BET, SEM and infrared spectroscopy techniques. The results confirmed the formation of Nano-MgO materials with crystallite size in range of 5-20 nm and surface areas of 336-556m^2/g. The product has been tested as destructive adsorbent for the decontamination of (2-chloroethyl) ethyl sulfide (2-CEES), a mimic of bis(2-chloroethyl) sulfide("HD" or Mustard Gas). Destructive adsorbent reaction has been carried out in heptanes and methanol media. The reaction was investigated by GC-FID and GC–MS techniques. Reaction rate in heptane has been observed to be higher than methanol. It seems a nonpolar media aided material transfer to the reactive surface sites without blocking them.
Keywords: *Nano-MgO, Decontamination, (2-chloroethyl) ethyl sulfide.*

1. INTRODUCTION

Surface of metal oxides play an important role in various reactions occurring in nature or in industrial processes. Metal oxides were found to be the promising adsorbent for the degradation of environmental pollutants both in normal and light irradiated conditions [1]. Its reactivity towards the toxic chemicals under normal conditions can be attributed to Lewis acid, Lewis base, Bronsted acid sites of varying coordination and the surface hydroxides [2-5]. Nano-MgO, CaO, ZnO and Al_2O_3 adsorb polar organics such as aldehydes, alcohols, ketones, and other polar organics in very high capacities, and substantially outperform the activated carbon samples that are normally employed for such purposes [1].
On the other hand, metal oxides have been established as the potential adsorbent material for the decontamination of chemical warfare agents (CWA) [5-10]. Due to their high surface area, large number of highly reactive edges, corner defect sites, unusual lattice planes and high surface to volume ratio, nanocrystalline metal oxides possess enhanced reactive properties towards chemical warfare agents and hence were successfully tested for the decontamination applications [11,12]. The adsorption ability of nanocrystalliane ionic metal oxides, in particular MgO, can be attributed to morphological feature–a high proportion of edge/corner sites available due to their polyhedral shapes. Both Lewis base and Lewis acid sites at edge/corner would be stronger due to coordinative unsaturation.
Indeed, models suggest that at least 20% of surface ions are positioned on edge/corner [13,14]. Furthermore, according to magnetic susceptibility studies, other types of surface defects such as ion vacancies, electron-deficient and electron-rich sites exist[1]. Nano-MgO is commonly obtained by

thermal decomposition of magnesium hydroxide or carbonate [15-17] and by a sol-gel process [18,19]. The oxide morphology, particle size and specific surface area depended on the preparation conditions (pH, gelling agent, calcinations rate and temperature) [20-25]. There is considerable interest in the synthesis of nanoscale magnesium oxide (MgO) particles via the magnesium alkoxide $Mg(OR)_2$ route. Generally, an alkoxide is hydrolyzed in an alcohol solvent to yield the hydroxide, which is followed by isolation and thermal dehydration [26,27].Stengl and co-workers [28] have described the preparation of magnesium hydroxide aerogels on the basis of the hydrolysis and condensation reactions of the alkoxide.

They carried out the hydrolysis of $Mg(OCH_3)_2$ in a water-methanol-toluene mixture and, after autoclave hypercritical drying, magnesium oxide aerogels were obtained with surface areas of about 537 m^2/g. The main aims of present research are to investigate the respective method and procedure of the nano-sized magnesium oxide preparation with high surface area and evaluate the prepared oxides for their respective detoxification activities. The detoxification activity of the prepared samples of Nano-MgO was evaluated by using HD-simulated 2-Chloroethyl ethyl Sulfide and identifies the destructive products.

2. EXPERIMENTAL

2.1. Material

Analytical grade methanol, n-heptane, n-octane, toluene, Commercial magnesium oxide (CM-MgO) with BET of 50 m^2/g and magnesium ribbon were purchased from Merck, 2-chloroethyl ethyl sulphide was Aldrich product.

2.2. Synthesis of Nano-MgO

A modified autoclave hypercritical procedure has been developed to prepare nano-MgO particles. This method has four steps: preparation of $Mg(OCH_3)_2$ by the reaction of magnesium metal with methanol(8% w/v), then hydrolysis of $Mg(OCH_3)_2$ in presence of toluene, after which the hydroxide gel was transferred to the reactor, and finally the reactor was pressurized with nitrogen gas to obtain the desired pressure of 110 psi. Then, the reactor was slowly heated to 275°C at a rate of 2°C/min for 2 hours. The temperature was allowed to equilibrate for 30 minutes at 275°C followed by a quick release of the pressure. The reactor was allowed to cool for 1 hour. The resulting product was a white to tan powder and stored in a vial in a desiccators for future use.

2.3. Characterization

XRD patterns were obtained in a Scintag-XDS 2000 diffractometer, the radition source used was CuKα radiation with applied voltage and current of 40 kV and 40mA, respectively. Two ɵ angles ranged from 10^o to 100^o at a speed of 2^o per minute. Scanning electron micrograph was obtained with a HITACHI S-300N instrumental. Surface area, was measured by the BET method [29] with a Quantachroma nova series 1200 instrument. Samples of 150 mg were heated under vacuum at the desired temperature, usually 300°C for several hours, followed by cooling and then performing the N_2 adsorption measurements at 77 K at different pressures. In order to identify the products from degradation of 2-CEES, n-heptane was used to extract the sample 2-CEES over the oxides.

The extractants were analyzed by HP-Agilen GC-MS system and Varian Star 3400 CX gas chromatography with flame ionization (FID) detector. A fused-silica capillary column DB-1701(30m×0.25mm×0.25µm) was chosen. The initial and final temperature of the oven was programmed 60°C (held for 6.00 min) and 200°C respectively, to reach the final temperature (after 6.00 min), the rate increasing temperature of 20°C /min was chosen. The separated products were identified by comparison of experimental mass spectra with references.

2.4. GC and GC-MS Studies.

The reaction was set up in a round bottom flask, 100 mg for Nano-MgO (or CM-MgO), 5µl 2-CEES, 5µl for n-octane (internal reference), 10 ml heptane (or methanol), under N_2 atmosphere and room temperature. The liquid fraction (10 µl) was drawn through a serum-septum periodically (5, 15, 30, 60, 120, 360, 720 min) and were directly injected on

column with a microliter syringe.

3. RESULTS AND DISCUSISION

3.1. Preparation of the nano-MgO with high surface area

Purity and structure of MgO powders determinated through X-ray diffraction (XRD) measurements. The most powerful aspect of XRD powder is that every solid crystalline compound has a characteristic ‘’fingerprint” even more important is the each crystal from of that compound also gives a distinctive pattern, which makes XRD powder an essential tool not only for identification of solids, but also for information about their crystal structures, packing and crystallite size. XRD of MgO is shown in Figure 1 for batch 6 (Table 1). Spectra were compared to the JCPDS (Joint Committee for Powder Diffraction Standards) files included in the software as standard references. The mean crystallite size of the nanocrystalline MgO materials was estimated by using Scherrer formula [30] and it was found to be in the rang of 4-20 nm, whereas it was 0.15 μm for the bulk materials (as per the catalogue). Figure 2 shows typical surface section SEM microghraph of obtained MgO powder (batch 6). Most of MgO particles are of a similar size.

Table1: *Specific surface area of MgO; methoxide solution/toluene solvent (M/S)*

batch	M/S	P_{N2}(psi)	S_{BET}(m^2/g)
1	50/100	0	218
2	50/100	110	336
3	50/100	220	340
4	40/100	110	425
5	30/100	110	500
6	20/100	110	556
7	15/100	110	540
8	10/100	110	535
9	20/100	0	366
10	20/100	220	546

Specific surface areas of ten batches of representative Nano-MgO precursors prepared under different experimental conditions are presented in Table 1. The data show extremely high specific surface areas, 218-556m^2/g, comparing with that of the commercial sample 50m^2/g. Indeed, the experimental condition used in our experiment was modified from that of Stengl and co-workers[28], magnesium oxide aerogels with surface areas of about 537 m^2/g, and such modification caused a great effect on the specific surface area of the resulting products. This improvement could result from two major factors. First, using an excess of toluene solvent could affect the hydrolysis-cocondensation process. As stated

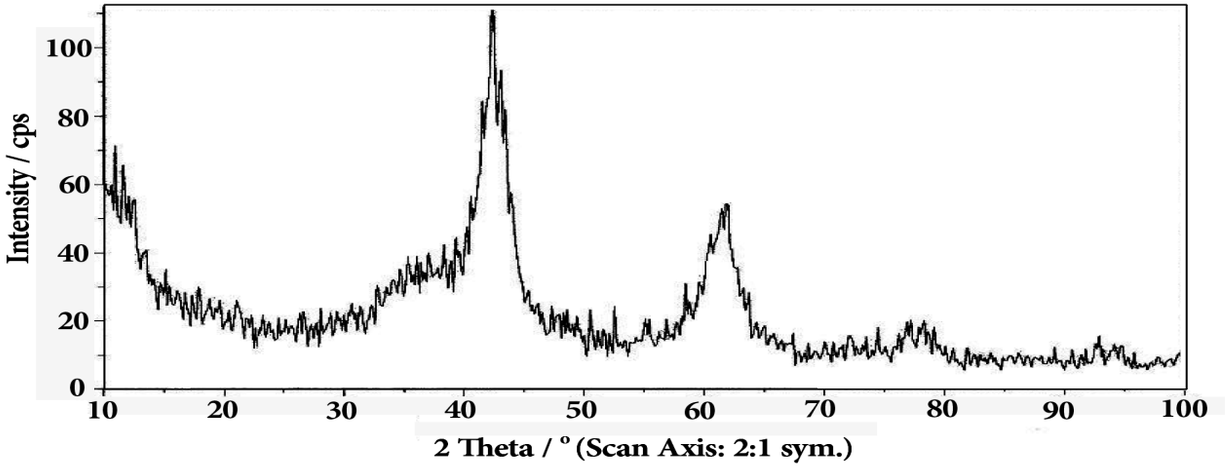

Figure 1: *X-Ray diffraction pattern of the synthesized of nano-Mgo (batch 6)*

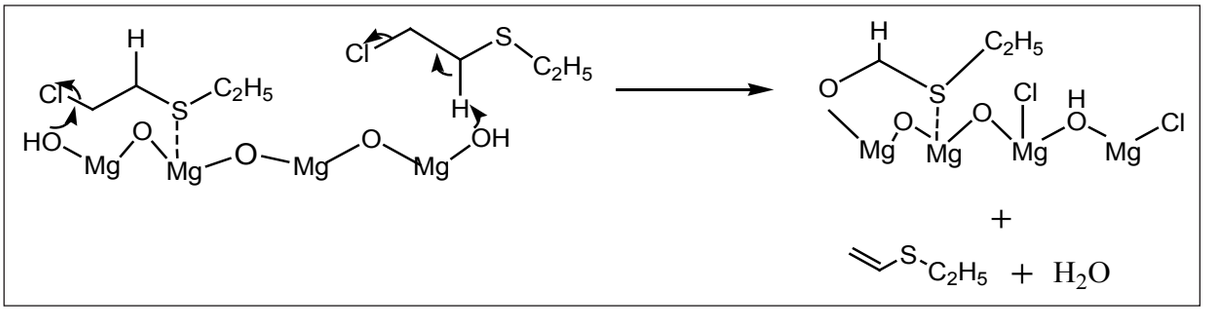

Scheme 1: *Elemination pathway for 2-CEES on MgO involving Mg^{2+} Lewis acid sites and surface-OH*

by Hubert-Pfalzgraf, the hydrolysis-polymerization reactions are governed by several parameters including solvent and dilution [31].

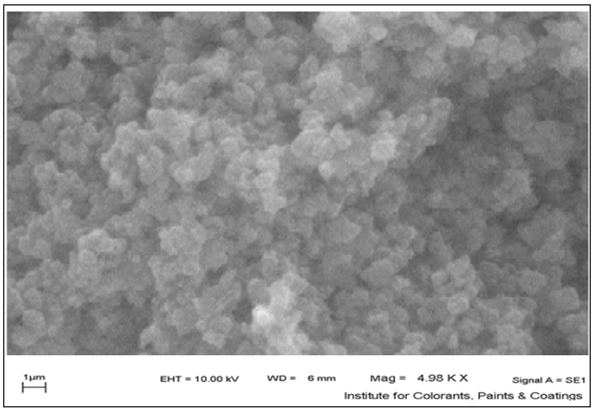

Figure 2: *SEM micrograph of the MgO batch 6*

The interaction between the OH group and toluene solvent, perhaps, could help to protect the gel structure. The incorporation of a hydrophobic organic solvent may reduce liquid-pore wall interaction, which is one of the major causes of the capillary force and the stress formation [32]. With increase toluene solvent was used, i.e. methoxide solution/toluene solvent (M/S), the surface area increased from 336 to 556 m^2/g. The use of M/S ratio, equal to 20/100 is seemed to yield the most optimize surface area (556 m^2/g) in field of our research.

The large excess amount of toluene solvent, i.e. M/S=15/100 and 10/100 solution, did not future improve the surface area of final product. Secondly, the introduction of nitrogen gas to the gel before the autoclave treatment could cause the shrinkage of the gel during the drying process. This effect was reported to be the case in the preparation of autoclave dried silica gel [33]. It was demonstrated that the application of an inert gas, N_2, in the autoclave provided a control of the shrinkage of the gels, a pressure of 80 bars was necessary to avoid any shrinkage. In our experiment, a pressure of 110 psi (7.5 bar) is the optimum condition. Application of higher pressure of N_2 at 220 psi (15 bar) does not improve the specific surface area of the product.

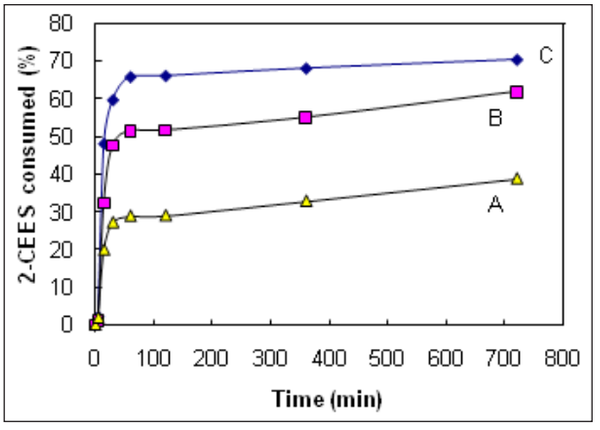

Figure 3: *The rate of disappearance of 2-CEES in heptane with Series of MgO varying surface areas; A:50 m^2/g; B:336 m^2/g; C:556 m^2/g.*

On the other hand, MgO samples were also characterized by FTIR which apparently shows the presence of hydroxyl group in surface of the product as depicted by the appearance of IR absorption peaks at 3431 cm^{-1}. In addition to this, Mg–O absorption at 540 cm^{-1} is also observed. As the material was calcinated at 500 °C and stored in air tight bottle, chances for the presence of moisture were negligible. FTIR spectrum of the synthesized

MgO (not shown here) is similar to the one reported in literature [34].

3.2. Reaction in heptane

The aim of this work was to demonstrate that the presence of solvent would greatly enhance the rate of the destructive adsorption process. Without solvent, the complete reaction can take days or weeks to complete [35]. Heptane was initially chosen as a solvent as it is considered to be inert and facilitates 2-CEES transfer to the MgO surface. Several preparative batches of Nano-MgO and 2-CEES adsorption reaction were studied in heptanes, for determent relation of MgO surface area and reaction rate (Table 1). The reaction rate of adsorption and decomposition of 2-CEES with MgO has been verified by GC during these reactions. We found that the reaction rate in heptane is directly related to the surface area of the Nano-MgO.

For example in Figure 3, over 59.6% of the 2-CEES was consumed with batch 6 (556 m^2/g surface area in 30 Min), less than 47.5% disappeared with batch 2 (336 m^2/g), and less than 27.1% disappeared with CM-MgO (50 m^2/g). However, note that CM-Mg, which is morphologically different [9,12], exhibits far lower rate. It is clear that crystal shape as well as surface area are effected in this reaction adsorbtion important.

Aerogel prepared-MgO crystallites are polyhedral, and CM-MgO is polycrystalline, mainly as cubes [9,10]. Actually, the initial rapid rate of these reactions markedly slowed after about 30 min, and this behavior has been observed earlier [4,9-12]. It is likely that an array of site reactivity is involved, and the most active sites are consumed first (edges, corners, defects), followed by the less reactive sites (such as planar surfaces). GC-MS analysis was carried out after 720 min of reaction start. Two peaks were eluted at 3.1 and 5.4 minutes. The eluents were fragmented using electron ionization. Figure 4 shows both products, 2-CEES has a molecular weight of 123 which matches the M peak, with M+2 from the ^{37}Cl isotopes, and the largest fragmentation at 123 from the loss of CH_2=Cl. This fragmentation matches up with a 2-CEES standard. The second spectra is attributed to ethyl vinyl sulfide, MW=88. Fragmentation peak, at 27 m/z, is C_2H_5-S from the loss of CH_2-CH*.

Suggest a MgO-2-CEES destructive adsorption reaction depicted in Scheme 1. Note the isolated OH groups working in tandem with non hydroxylated MgO moieties (thus Mg^{2+} ion binds to the sulfur of 2-CEES) could lead to the bound substitution

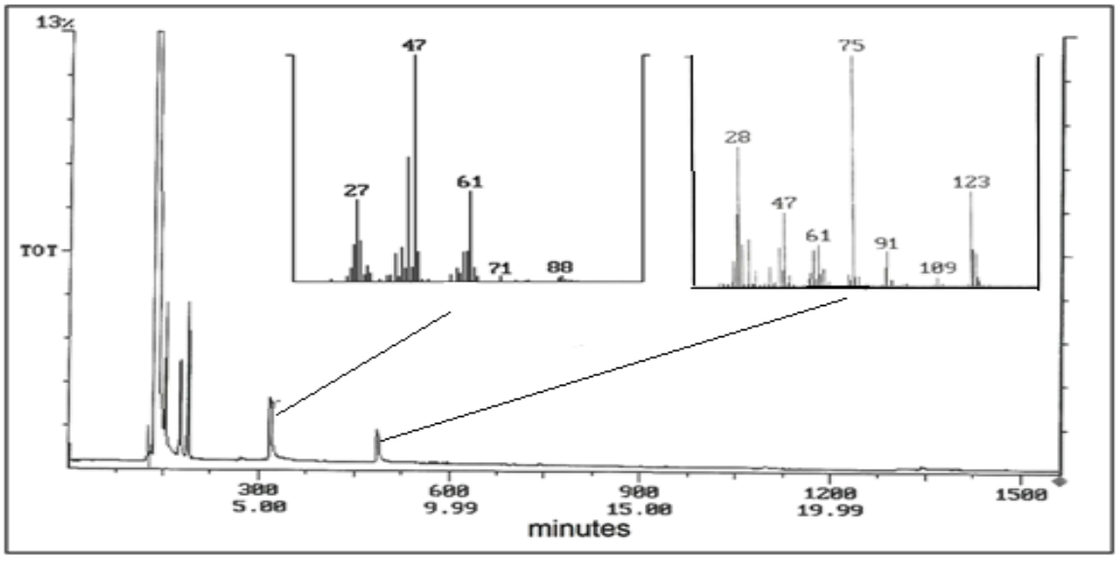

Figure 4: *GC-MS of 2-CEES and product elimination of reaction MgO with 2-CEES in heptane.*

(alkoxide) product. For the vinyl product formation, it may be due to the isolated OH groups which are capable of causing E2 elimination as shown in Scheme 1.

3.3. Reaction in methanol

With methanol the results were very different from those in heptane. The amount of 2-CEES consumed in heptane was two to three times greater over the same period of time. The results with methanol show, however, that polar solvent hinder the reaction, even though polar reaction transition state must be involved.

These data indicate that polar solvent can compete with reactive sites on the MgO surface, including Bronsted acid and Lewis acid sites. In particular, the blocking of Lewis acid site would hinder the coordination of the 2-CEES. Since methanol is such a strong hindrance to the reaction, this tends to lend further support to the idea that methanol simply blocks access to the sorbent surface. The formation of substitution product (likely in the deported alkoxide state) could not follow by GC during this reaction, because substitution product bonded very strongly to the surface [7]. Narske and his co-workers [34] reported similar result when working with CaO reaction with 2-CEES.

4. CONCLUSION

In the present study, nano-MgO was prepared by sol–gel method with crystallite size in range of 5-20 nm and surface areas of 336-556m^2/g. The data show extremely high specific surface areas, compared with the work of Stengl [28]. This may be duo to two major factors. Firstly, the use of an excess amount of toluene solvent may affect the hydrolysis-cocondensation process.

Secondly, the introduction of nitrogen gas to the gel before the autoclave treatment may cause shrinkage of the gel during the drying process. The amount of 2-CEES consumed with heptane was two to three times greater than that with methanol over the same period of time. Polar solvent can compete with reactive sites on the MgO surface, thus; blocking the Lewis acid site which may hinder the coordination of 2-CEES. The results show that nano-MgO with high specific surface areas can be effectively used for decontaminating (2-chloroethyl) ethyl sulfide.

REFERENCE

1. J. A. Rodriguez, Fernandez-Garcia M., Synthesis, Properties and Applications of Oxide Nanomaterials; John Wiley & Sons, New Jersey, 2007.
2. C. F. Richard, J. F. Bosquet, J. Pilichowski, Photochem Photobiol A: Chem. Vol. 108, (1997), p. 45.
3. M. D. Driessen, T. M. Miller, V. H. Grassian, J. Mol. Catal A: Chem. Vol. 131, (1998), p. 149.
4. Saxena, A. Srivastava, A. Sharma, B. Singh, J. Hazard. Mater. Vol. 112, (2009), p. 419.
5. M. C. Yeber, J. Rodriguez, J. Freer, N. Durian, H. D. Mansilla, Chemosphere. Vol. 41, (2000), p. 1193.
6. G. M. Medine, V. Zaikovski, K. J. Klabunde, J. Mater. Chem. Vol. 14, (2004), p. 757.
7. Y. Diao, W. P. Walawender, C. M. Sorenson, K. J. Klabunde , T. Ricker, Chem. Mater. Vol. 14, (2002), p. 362.
8. G. W. Wagner, O. Koper, E. Lucas, S. Decker, K. J. Klabunde, J. Phys. Chem. B, Vol. 104, (2000), p. 5118.
9. Rajagopalan S, Koper O, Decker S, Klabunde K J, *Chem Eur J*, Vol. 8, (2002), p. 2602.
10. G. K. Prasad, T. H. Mahato, B. Singh, K. Ganesan, P. Pandey, K. Sekhar, J Hazard Mater. Vol. 149, (2007), p. 460.
11. G. W. Wagner, P. W. Bartram, O. Koper, K. J. Klabunde, J. Phys. Chem. B, Vol. 103, (1999), p, 3225.
12. G. W. Wagner, L. R. Procell, R. J. O,Connor, S. Munavalli, C. L. Carnes, P. N. Kapoor , K. J. Klabunde, J. Am. Chem. Soc. Vol. 123, (2001), p. 1636.
13. L. Interrante, M. Hampden-smith, Chemistry of Materials, Wiley-VCH, (1998), pp. 271-327.
14. K. Klabunde, J. V. Stark, O. Koper, C. Mohs, D. G. Park, S. Decker, Y. Jiang, I. Lagadic, D. Zhang, J. Phys. Chem. Vol. 100, (1996), pp. 12142.

15. Jeevanandam P and Klabunde K J, Langmuir, Vol. 18, (2002), p. 5309.

16. D. R. Lide, CRC Handbook of Chemistry and Physics. A Ready-Reference Book of Chemical and Physical Data, 77th Edition, CRC Press, Boca Raton - New York -London - Tokyo. 2004.

17. M. A. Aramendia, V. Borau, C. Jimenez, J. Mater. Chem. Vol. 6, (1996), p. 1943.

18. B. Q.Xu, J. M. Wei, H. Y. Wang, Catal Today, Vol. 68, (2001), p. 217.

19. H. S. Choi, S. T. Hwang, J. Mat. Res. Vol. 15, (2000), p. 842.

20. T. Lopez, R. Gomez, J. Navarrete, E. Lopez-Salinas, J. Sol-Gel Sci. Tech. Vol. 13, (1998), p. 1043.

21. S. Utamapanya, K. J. Klabunde , J. R. Schlup, Chem. Mater. Vol. 3, (1991), p. 175.

22. Z. Cheng, H. Tang, H. Zhu, H. Zuo, G. Zhang, Appl. Cat. B. Eev. Vol. 79, (2008), p. 323.

23. H. Zhao, K.Y. Robert, Key Eng. Mat. Vol. 334 (2007), p. 617.

24. L. Znaidi, K. Chhor, C. Pommier, Mat. Res. Bull. Vol. 31, (1996), p. 1527.

25. O. B. Koper, I. Lagadic, A. Volodin , K. Klabunde, J. Chem. Mater. Vol. 9, (1997), p. 2468.

26. T. Hattori, H. Matsumoto, J. Mohri, J. Mater. Sci. Lett. Vol. 2, (1983), p. 503.

27. P. J.Anderson, Horlock R F, Trans Faraday Soc. Vol. 58, (1962), p. 1993.

28. V. Štengl , S. Bakardjieva, M. Maříková, J. Šubrt, F. Opluštil, M. Olšanská, Cent. Eur. J. Chem. Vol. 2, (2004), p. 16.

29. J. R.Anderson, A. Khaleel, D. Park, High. Temp. Mater. Sci. Vol. 33, (1995), p. 99.

30. Cullity B D, Elements of X-Ray Diffraction 2nd ed., Addison-Wesley Publishing Company Inc., California, (1978), p. 102.

31. L. G.Hubert-Pfalzgraf, New. J. Chem. Vol. 11, (1987), p. 663.

32. H. Schmidt, J. of Non-Cryst Solids, Vol. 100, (1988), p. 51.

33. C. AM. Mulder, J. G.Van Lierop, International Symposium on Aerogels in Würzburg, Sept. 23-25, 1985.

34. R. M. Narske, K. J. Klabunde, S. Fultz, Langmuir. Vol. 18, (2000), p. 4819.

35. K. J. Klabunde, Nanoscale Materials in Chemistry, Wiley Interscience, New York, NY, 2001.

Synthesis of magnetron sputtered WOâ‚ƒ nanoparticles-degradation of 2-chloroethyl ethyl sulfide and dimethyl methyl phosphonate.
Authors: Monu Verma Ramesh Chandra Vinod Kumar Gupta.Â In the present study, tungsten oxide nanoparticles were synthesized using DC magnetron sputtering and investigated their potential for decontamination of 2-chloroethyl ethyl sulfide (CEES) and dimethyl methyl phosphonate (DMMP). The tungsten oxide nanoparticles were characterized by Powder XRD, FE-SEM, EDS, TEM, TGA, N2-BET and FT-IR techniques. The XRD patterns of as-deposited and post annealed tungsten oxide nanoparticles reveal that the crystallite size of detected monoclinic phase WO3 nanoparticle was increased with increasing annealing temperatures.